



HAL
open science

Longitudinal study of functional brain network reorganization in clinically isolated syndrome

Ismail Koubiyr, Mathilde Deloire, Pierre Besson, Pierrick Coupé, Cécile Dulau, Jean Pelletier, Thomas Tourdias, Bertrand Audoin, Bruno Brochet, Jean-Philippe Ranjeva, et al.

► To cite this version:

Ismail Koubiyr, Mathilde Deloire, Pierre Besson, Pierrick Coupé, Cécile Dulau, et al.. Longitudinal study of functional brain network reorganization in clinically isolated syndrome. *Multiple Sclerosis Journal*, 2018, 26 (2), pp.135245851881310. 10.1177/1352458518813108 . hal-02059512

HAL Id: hal-02059512

<https://amu.hal.science/hal-02059512>

Submitted on 25 Apr 2022

HAL is a multi-disciplinary open access archive for the deposit and dissemination of scientific research documents, whether they are published or not. The documents may come from teaching and research institutions in France or abroad, or from public or private research centers.

L'archive ouverte pluridisciplinaire **HAL**, est destinée au dépôt et à la diffusion de documents scientifiques de niveau recherche, publiés ou non, émanant des établissements d'enseignement et de recherche français ou étrangers, des laboratoires publics ou privés.

Longitudinal study of functional brain network reorganization in clinically isolated syndrome

Ismail Koubiyr^{1,2}; Mathilde Deloire³; Pierre Besson^{5,6}; Pierrick Coupé⁴; Cécile Dulau³; Jean Pelletier^{5,6,7}; Thomas Tourdias^{1,2,3}; Bertrand Audoin^{5,6,7}; Bruno Brochet^{1,2,3}; Jean-Philippe Ranjeva^{5,6}; Aurélie Ruet^{1,2,3}

Affiliations

¹ Univ. Bordeaux, F-33000 Bordeaux, France

² Inserm U1215 - Neurocentre Magendie, F-33000 Bordeaux, France

³ CHU de Bordeaux, F-33000 Bordeaux, France

⁴ Laboratoire Bordelais de Recherche en Informatique, UMR CNRS 5800, PICTURA, F-33405 Talence, France

⁵ AixMarseille Univ, CNRS, CRMBM UMR 7339, Marseille, France

⁶ AixMarseille Univ, APHM, Hopital la Timone, CEMEREM, Marseille, France

⁷ APHM, Hopital la Timone, service de Neurologie, Marseille, France

Corresponding Author

Pr. Bruno Brochet

CHU Pellegrin,

Place Amélie Raba Léon

33000 Bordeaux, France

Phone +33556795679

bruno.brochet@chu-bordeaux.fr

Key words: multiple sclerosis, clinically isolated syndrome, functional MRI, longitudinal, graph theory, networks

Number of tables: 2

Number of colored figures: 5

Word count abstract: 199

Word count paper: 3000

References: 33

Abstract

Background: There is a lack of longitudinal studies exploring the topological organization of functional brain networks at the early stages of multiple sclerosis (MS).

Objectives: This study aims to assess potential brain functional reorganization at rest in patients with CIS (PwCIS) after one year of evolution and to characterize the dynamics of functional brain networks at the early stage of the disease.

Methods: We prospectively included 41 PwCIS and 19 matched healthy controls (HC). They were scanned at baseline and after 1 year. Using graph theory, topological metrics were calculated for each region. Hub disruption index was computed for each metric. **Results:** Hub disruption indexes of degree and betweenness centrality were negative at baseline in patients ($p < 0.05$), suggesting brain reorganization. After 1 year, hub disruption indexes for degree and betweenness centrality were still negative ($p < 0.00001$), but such reorganization appeared more pronounced than at baseline. Different brain regions were driving these alterations. No global efficiency differences were observed between PwCIS and HC either at baseline or at 1 year.

Conclusion: Dynamic changes in functional brain networks appear at the early stages of MS and are associated with the maintenance of normal global efficiency in the brain, suggesting a compensatory effect.

Introduction

Patients with a first neurological episode of the type seen in multiple sclerosis (MS), so-called clinically isolated syndrome (CIS) are at a high risk of progressing to MS.¹ Multiple sclerosis pathology is characterized by inflammation, demyelination, axonal injury and axonal loss.² This pathology induces disruptions in brain connectivity, which can lead to sensory³, motor⁴ or cognitive^{5,6} dysfunction. Some studies have shown that functional compensatory mechanisms occurring at the early stages of the disease can limit these clinical manifestations.⁷⁻⁹ Resting-state functional imaging studies in MS have shown the potential to non-invasively map the intrinsic functional brain networks and to detect early functional brain changes.^{6,10-12} Furthermore, graph theory has proved to depict the topological organization of the brain by visualizing the overall connectivity patterns and by characterizing the brain's global organization.¹³ Recent studies investigated brain network topology at the CIS stage. Liu et al. (2016)¹⁴ showed decreased nodal efficiency in the superior temporal gyrus, left rolandic operculum and left insula, while Shu et al. (2016)¹⁵ did not notice any local changes in the functional connectome of CIS patients. This lack of network changes was then thought to be due to subtle functional changes during this very early stage of the disease. To the best of our knowledge, these graph-based functional studies of CIS were only performed cross-sectionally; therefore, they did not provide answers regarding the dynamics of the functional brain networks at this stage.¹⁶ In MS, both increased and decreased centrality have been observed in different parts of the brain.^{6,11,17} Faivre et al. (2016)¹⁸ studied the evolution of network topology over 2 years of follow-ups in relapsing-remitting MS (RRMS) patients after on average 10 years of evolution of the disease. At baseline, the local and nodal efficiencies were higher in patients compared to controls, while after 2 years, these values were decreased and were no longer different from controls. Thus, the authors hypothesized that the compensatory mechanisms failed after reaching a maximal level. In this context, one may

wonder whether such compensatory mechanisms (or failure of compensation) could be involved as early as at the stage of CIS.

For such needs, we aimed to study resting-state functional brain network topology longitudinally, few months after CIS and one year after using both global and local graph-based measures to assess functional brain network reorganization.

Materials and methods

Standard protocol, approvals, registration and patient consent

Each participant gave written informed consent. The patients were included in a prospective study without intervention, analyzing early brain damage in patients with CIS (PwCIS) (SCICOG, ClinicalTrials.gov Identifier: NCT01865357). This study was approved by the local ethics committee.

Participants

Fifty-two PwCIS were prospectively recruited less than 6 months after a first neurological episode of the type seen in MS and presented with at least two clinically silent cerebral lesions on fast fluid-attenuated inversion recovery (FLAIR) images characteristic of MS. All patients underwent an MRI scan at baseline, and forty-one PwCIS were rescanned 1 year after the first assessment. The exclusion criteria included under 18 years of age, the inability to perform the MRI, a history of other neurological or psychiatric disorders, an MS attack within the 2 months prior to the screening, corticosteroid pulse therapy within the 2 months prior to the screening and severe depression (Beck Depression Inventory score (BDI) > 27). Clinical assessments and the Expanded Disability Status Scale (EDSS) scores were determined by expert neurologists.

Twenty healthy controls (HC) matched for age, sex and educational level were also included and underwent the same MRI protocol. Nineteen of these HC were rescanned within one year of the first assessment. Because our aim was to study the longitudinal evolution of brain

network topology, only participants with longitudinal follow-ups were considered for the current analyses. Therefore, the 41 patients and the 19 HC followed over 1 year are referred to as PwCIS and HC, respectively.

All participants were also evaluated using a large neuropsychological (NP) battery detailed in supplementary material.

MRI acquisition

The MRI acquisition was performed on a 3T MRI system (Achieva TX system, Philips Healthcare, Best, The Netherlands; Signa, GE Healthcare, Discovery MR 750w, Milwaukee, Wisconsin). The acquisition protocol was harmonized between the magnets and consisted of a three-dimensional (3D) T1-weighted sequence using magnetization prepared rapid gradient echo (MP-RAGE) imaging, a two-dimensional (2D) FLAIR sequence, and resting-state functional MRI was obtained with an echo-planar imaging (EPI) sequence. See supplementary material for technical details.

fMRI preprocessing

Using Statistical Parametric Mapping (SPM12, www.fil.ion.ucl.ac.uk/spm), we followed the same fMRI preprocessing that was used in a previous study¹⁹. Preprocessing steps are detailed in supplementary material.

Structural preprocessing and regions of interest

Briefly, lesions were segmented on FLAIR data and lesion filling was applied to T1-weighted images. Structural data were preprocessed with FreeSurfer (v5.3) leading to a custom-made atlas of 83 regions per hemisphere. Details are available in supplementary material.

Network construction

Interactions between brain regions can be described by graph theoretical methods²⁰. These methods represent interactions consisting of nodes (brain regions) and links/edges between the nodes (functional interaction). To construct functional connectivity networks, for each

participant, the average BOLD time courses were extracted from each one of the 166 regions defined by our final atlas. Then, Pearson's linear correlation coefficients were computed between the signals from all pairs of regions. It led to an individual-level square 166x166 correlation matrix. We created an adjacency matrix with the same number of edges among participants. To do this, we performed proportional thresholding so that each correlation was retained and set to 1 if superior to that threshold or set to 0 otherwise. We assessed the networks over a wide range of density thresholds (5-20%). Our results were considered robust when they were identical across these different densities. To simplify, we only show the results for a 15% density threshold. This choice was based on priors relative to the known sparsity of the anatomical connections in the human nervous systems^{18,20}. The brain connectivity toolbox (brain-connectivity-toolbox.net)²¹ was used to calculate the following connectivity measures:

Degree (Deg) represents the number of links connected to a node

$$k_i = \sum_{j \in N} a_{ij}$$

where a_{ij} is the connection status between i and j : $a_{ij} = 1$ when link (i, j) exists (when i and j are neighbors); $a_{ij} = 0$ otherwise.

Local efficiency (Eloc)²² represents the short-range connectivity and is related to the density of the short-distance connections of the network. Eloc shows the information transfer in the immediate neighborhood of each node

$$Eloc_i = \frac{1}{n} \sum_{i \in N} \frac{\sum_{j, h \in N, j \neq i} a_{ij} a_{ih} [d_{jh}(N_i)]^{-1}}{k_i(k_i - 1)}$$

where $Eloc_i$ is the local efficiency of node i , and $d_{jh}(N_i)$ is the length of the shortest path between j and h that contains only neighbors of i .

Global efficiency (Eglob)²² of the network

$$E_{glob} = \frac{1}{n} \sum_{i \in N} \frac{\sum_{j \in N, j \neq i} d_{ij}^{-1}}{n-1}$$

where d_{ij} is the shortest path length between nodes i and j .

Betweenness centrality (BCN)²³ represents a measure of ‘hubness’, and generally speaking corresponds to brain areas that have the highest connectivity and form the core of the brain network

$$BCN_i = \frac{1}{(n-1)(n-2)} \sum_{h,j \in N, h \neq j, h \neq i, j \neq i} \frac{\rho_{hj}(i)}{\rho_{hj}}$$

where ρ_{hj} is the number of shortest paths between h and j , and $\rho_{hj}(i)$ is the number of shortest paths between h and j that pass through i .

We first assessed the global brain reorganization using the hub disruption indexes (κ)^{24,25} for Deg, Eloc and BCN. The hub disruption indexes measured the way the network’s nodes were radically reorganized in comparison with healthy volunteers, with increased hubness in some regions and decreased hubness in others. To compute κ , we first subtracted the HC group mean network metric of the same node from a patient before we plotted the difference against the HC group mean. κ is the gradient of a straight line fitted to these data. In other words, for each subject and each measure, this gradient was estimated as the slope of the following graph:

$$(Measure_{subject} - Measure_{\mu Controls}) = f(Measure_{\mu Controls})$$

where $\mu Controls$ is the mean value across the whole HC group. Figure 1 illustrates the hub disruption index calculation for both a representative patient and a healthy volunteer. In other words, this metric can be used to compare the behavior of the network of a single subject with respect to a referential network topology (the normative network topology of a healthy control group).

Statistical analysis

The statistical analyses were performed using SPSS software version 23.0 (SPSS, Chicago, IL, USA).

Parametric and non-parametric tests were used according to the variables distribution.

Normality of the distribution was assessed using the Shapiro-Wilk test. The categorical variables were investigated with χ^2 tests. Cross-sectional comparisons were performed using two sample t-tests (normally distributed data) and Mann-Whitney U tests (non-normal data), while longitudinal comparisons used paired t-tests (normally distributed data) or Wilcoxon tests (non-normal data).

The hub disruption indexes for each metric were investigated using one-sample t-tests. If it was significantly different from zero indicating a global reorganization, a region-wise comparison for the correspondent metric was used to look for the major regions driving this reorganization. This comparison was done using a Mann-Whitney U test and was corrected for multiple comparisons using the false discovery rate (FDR).

The p-value < 0.05 was considered statistically significant.

Results

Clinical and conventional MRI characteristics

The characteristics of PwCIS and HC at both time-points are reported in Table 1.

The groups were matched for age, gender and educational level.

In patients, EDSS scores did not change significantly between baseline (median EDSS = 1, range = 0-3) and year 1 (median EDSS = 1, range = 0-5), and T2 lesion volumes (T2 LV) did not differ significantly between baseline (median T2 LV = 0.98 ml, range = 0.02-63.12) and year 1 (median T2 LV = 1.32 ml, range = 0.07-67.74).

Only a moderate cognitive impairment was noticed at baseline, as only the computerized speed cognitive test (CSCT) and the brief visual memory test revised (BVMTR) were altered

(see Table S.1). This cognitive impairment was no longer observed after 1-year as PwCIS showed no significant differences compared to HC (see Table S.2).

Brain network reorganization at baseline

The PwCIS showed significant brain network reorganization, in that the hub disruption indexes for degree and betweenness centrality were significantly negative ($p < 0.001$ and $p < 0.05$, respectively) (Figure 2). However, their global efficiencies were not different compared to the HC (0.525 ± 0.013 vs 0.533 ± 0.012). The hub disruption index of the local efficiency was not significantly different from 0.

Brain network reorganization at 1 year

Functional brain reorganization was still present at the 1-year follow-up in PwCIS, as the hub disruption indexes for degree and betweenness centrality were still significantly negative ($p < 0.00001$ for both comparisons) (Figure 3). Patients were still able to maintain their global efficiency, as it was not different compared to the controls (0.525 ± 0.017 vs 0.522 ± 0.025). As was the case at baseline, the hub disruption index for local efficiency was not significantly different from 0. When comparing these network parameters between converters to MS and CIS, no significant differences were noticed.

To assess the longitudinal evolution of these hub disruption indexes, a paired t-test comparison was used for degree and betweenness centrality at both time-points. The hub disruption indexes of degree and betweenness centrality were both significantly lower at year 1 compared to baseline (-0.30 ± 0.55 at baseline vs -0.65 ± 0.60 at year 1 for degree, $p < 0.001$; -0.00005 ± 0.00014 at baseline vs -0.0002 ± 0.00014 at year 1 for betweenness centrality, $p < 0.00001$, respectively).

Regional modifications

Both the degree and betweenness centrality showed significantly negative hub disruption indexes at both time-points in PwCIS, indicating global brain reorganization. To assess the

major regions driving this reorganization, region-wise comparisons were performed for these two metrics.

To qualitatively assess the topography of the brain network reorganization in PwCIS for both the degree and betweenness centrality, we displayed on surface renderings the regions showing abnormal connectivity compared to the HC before multiple comparison correction (Figures 4, 5 and Table 2).

In regard to betweenness centrality, no region survived the multiple comparison correction at either time-points.

In regard to degree, the right middle temporal gyrus showed significantly more connections in PwCIS compared to HC at baseline. One year after, the bilateral hippocampus and the post-ventral cingulate gyrus, as well as the left parieto-occipital sulcus, exhibited significantly higher degrees in PwCIS than in controls, while the right middle occipital gyrus and the left posterior segment of the lateral fissure had lower connections.

Hub disruption index and clinical outcomes

To assess whether brain reorganization at this stage of the disease is related to disability (EDSS) or to the patient's lesion load (LL), the hub disruption indexes of degree and betweenness centrality were correlated to EDSS scores and LL using the Spearman rank correlation coefficient. Both the EDSS scores and LL did not show any significant correlations with the altered hub disruption indexes, either at baseline or 1-year after.

Then, Pearson correlation was used between altered cognitive tests and corresponding hub disruption indexes. Hub disruption index of betweenness centrality was observed to be correlated to delayed recall of the BVMTR (BVMTR-DR) as $r = -0.32$ and $p < 0.05$ at 1-year.

This indicates a more pronounced brain network reorganization as the cognitive performances are getting better.

Discussion

In the current study, we investigated, for the first time, the longitudinal topological reorganization of functional brain networks in PwCIS. We found that brain network reorganization began at the onset of the disease and evolved over the first year. However, global brain function preservation and normal cognitive performances indicate here a compensatory mechanism that is effective over this one year follow-up.

At baseline, we noticed the first hubness reorganization as the hub disruption indexes for both degree and betweenness centrality were significantly negative in PwCIS, which indicated a combination of underconnected and overconnected brain regions. This was mainly driven by an increased degree, which indicated the development of new connections, in the right middle temporal gyrus in PwCIS compared to HC. At this stage, the global efficiency of the brain in the PwCIS was still normal compared to HC, and PwCIS had only a moderate cognitive alteration at this stage. One year later, this brain network reorganization was even more pronounced. The hub disruption indexes for degree and betweenness centrality were significantly negative in the PwCIS but were also significantly lower than their baseline values, indicating an increased reorganization. Regionally, this reorganization was characterized by an increased degree in the bilateral hippocampus, the bilateral posterior cingulate gyrus and the left parieto-occipital sulcus. On the other hand, a decreased degree was observed in the right middle occipital gyrus and the left posterior segment of the lateral fissure. A preserved global efficiency with normal cognitive performances suggest a compensatory mechanism at this early stage, a hypothesis which was also sustained by the association of better visuo-spatial episodic memory performances with more pronounced brain network reorganization.

A few cross-sectional studies have assessed functional brain reorganization in CIS. Using a relatively small population of 14 CIS with a median disease duration of 1.4 years, Roosendaal et al. (2010)²⁷ observed increased functional synchronization in the posterior cingulate gyrus

in CIS patients, as well as in other resting-state networks (the executive function network, attention system and sensorimotor function network). Recently, Liu et al. (2016)¹⁴ investigated a population of 34 CIS with shorter disease duration (median disease duration of 1 month) and found a decrease in the nodal efficiency of the left rolandic operculum in CIS, which was in line with our findings of a decrease in the degree in the left posterior part of the lateral fissure. They also showed a decrease in the nodal efficiency of the insula and the superior temporal gyrus. These heterogeneous findings may be due to the inclusion of different sample sizes, disease durations or disability levels.

In clinically definite MS after years of evolution, increased functional connectivity was detected as a possible compensatory mechanism,^{4,6,10,11,17,28} while, decreased functional connectivity as a probable consequence of maladaptive reorganization due to acute or chronic inflammation, was also detected.^{6,11,17}

All together, these results suggested network alterations predominantly in the sensorimotor cortex, cingulate and fronto-temporal regions, as well as in the thalamus.^{6,10,11,17}

Furthermore, most studies have been performed cross-sectionally, which limits the understanding of the dynamics of brain network reorganization in MS and, more specifically, at the first stages of the disease. In the only longitudinal study performed in RRMS patients, Faivre et al. (2016)¹⁸ reported higher nodal and local efficiencies in patients than in controls at baseline. Two years later, these values decreased and were no longer different from controls, suggesting a primary compensatory mechanism followed by a brain functional connectivity depletion as the disease progresses.

Functional connectivity changes can be associated with a compensatory mechanism, as well as with maladaptive network rearrangements due to the loss of different large-scale cortical dynamics or the expression of between-network vulnerability.²⁹⁻³¹ A recent study showed the complex involvement of functional connectivity alterations, as they can be seen as

compensatory but are not limited to that.³² For example, an attempt to compensate after an acute lesion was shown,³³ while increased functional connectivity in CIS without conventional brain lesions was also associated to a high risk to develop MS.³⁴ In our case, the global efficiency preservation of our CIS population relative to HC and their normal cognitive performances, indicating normal brain functioning, suggest a compensatory mechanism at this early stage of the disease. This finding is in line with a task fMRI study in PwCIS, showing improvements in the patients' PASAT scores depending on their ability to recruit more compensatory mechanisms involving the right lateral prefrontal cortices (LPFC)³⁵.

This current study was not without limitations. The examination of network characteristics might have been influenced by the choice in the parcellation scheme.³⁶ Even though the organizational principles of functional brain networks seem to be independent of the selected parcellation method, our quantitative measures might have been modulated. Also, nonstationarity of brain connections is often disregarded as it is the case in our study, only the most robust effects in the steady state are captured. This leaves unknown transient states in network connectivity that may better explain how brain networks adapt to challenge and disruption.³⁷

In conclusion, the current study demonstrated, longitudinal brain network reorganization in patients with CIS. The pattern of functional connectivity reorganization remains the same during the first year after CIS but tends to be more pronounced at one year. In patients, regional reorganization of the connectivity was associated with the maintenance of normal global efficiency in the brain and normal cognitive and functional (EDSS) performances suggesting a compensatory effect. These findings provided new insights into the understanding of the underlying mechanisms and evolution of the disease. Further follow-ups with this cohort will be analyzed in order to generate a long-term model of brain network reorganization in MS.

Acknowledgments: The authors thank the neurologists of the AQUISEP network for their involvement in recruiting patients. The authors thank Dr. JC Ouallet, Dr. A Moroso and Dr. P Louiset for referring patients to the study. This work has been performed with the help of the French Observatoire of Multiple Sclerosis (OFSEP), which is supported by a grant provided by the French State and handled by the “Agence Nationale de la Recherche,” within the framework of the “Investments for the Future” program, under the reference ANR-10-COHO-002.

Funding: This study was supported by ANR-10-LABX-57 Translational Research and Advanced Imaging Laboratory (TRAIL), laboratory of excellence. The SCICOG study was also supported by a grant from Teva and ARSEP (Fondation ARSEP pour la recherche sur la sclérose en plaques).

Disclosures:

Ismail Koubiyr – PhD grant from TRAIL.

Mathilde Deloire – Nothing to disclose.

Pierre Besson – Nothing to disclose.

Pierrick Coupé – Nothing to disclose.

Cécile Dulau – received a speaker fee from BIOGEN.

Jean Pelletier – reports consulting fees and travels from Biogen, Sanofi-Genzyme, Novartis, Teva, Merck-Serono, Roche, Medday and unconditional research grants from Biogen, Novartis, Roche and Merck-Serono.

Thomas Tourdias – Nothing to disclose.

Bertrand Audoin – Nothing to disclose.

Bruno Brochet – Pr Brochet has received consultancy fees, speaker fees, research grants (non-personal), or honoraria from Novartis, BiogenIdec, Merck, Bayer Schering, Roche, Medday, Bayer, Actelion, Teva and Genzyme Sanofi outside the submitted study.

Jean Philippe Ranjeva – Nothing to disclose.

Aurélié Ruet – has received consultancy fees, speaker fees, research grants (nonpersonal), or honoraria from Novartis, BiogenIdec, Roche, Teva and Merck outside the submitted study.

References

1. Polman CH, Reingold SC, Banwell B, et al. Diagnostic criteria for multiple sclerosis: 2010 Revisions to the McDonald criteria. *Ann Neurol* 2011; 69: 292–302.
2. Zipp F, Gold R, Wiendl H. Identification of Inflammatory Neuronal Injury and

- Prevention of Neuronal Damage in Multiple Sclerosis. *JAMA Neurol*. Epub ahead of print 21 October 2013. DOI: 10.1001/jamaneurol.2013.4391.
3. Basile B, Castelli M, Monteleone F, et al. Functional connectivity changes within specific networks parallel the clinical evolution of multiple sclerosis. *Mult Scler J* 2014; 20: 1050–1057.
 4. Dogonowski AM, Siebner HR, Soelberg Sørensen P, et al. Resting-state connectivity of pre-motor cortex reflects disability in multiple sclerosis. *Acta Neurol Scand* 2013; 128: 328–335.
 5. Gamboa OL, Tagliazucchi E, Von Wegner F, et al. Working memory performance of early MS patients correlates inversely with modularity increases in resting state functional connectivity networks. *Neuroimage* 2014; 94: 385–395.
 6. Rocca MA, Valsasina P, Meani A, et al. Impaired functional integration in multiple sclerosis: a graph theory study. *Brain Struct Funct* 2016; 221: 115–131.
 7. Pantano P, Iannetti GD, Caramia F, et al. Cortical motor reorganization after a single clinical attack of multiple sclerosis. *Brain* 2002; 125: 1607–1615.
 8. Mainero C, Caramia F, Pozzilli C, et al. fMRI evidence of brain reorganization during attention and memory tasks in multiple sclerosis. *Neuroimage* 2004; 21: 858–867.
 9. Audoin B, Van Au Duong M, Ranjeva JP, et al. Magnetic resonance study of the influence of tissue damage and cortical reorganization on PASAT performance at the earliest stage of multiple sclerosis. *Hum Brain Mapp* 2005; 24: 216–228.
 10. Faivre A, Rico A, Zaaraoui W, et al. Assessing brain connectivity at rest is clinically relevant in early multiple sclerosis. *Mult Scler J* 2012; 18: 1251–1258.
 11. Schoonheim MM, Geurts JJG, Wiebenga OT, et al. Changes in functional network centrality underlie cognitive dysfunction and physical disability in multiple sclerosis. *Mult Scler J* 2014; 20: 1058–1065.

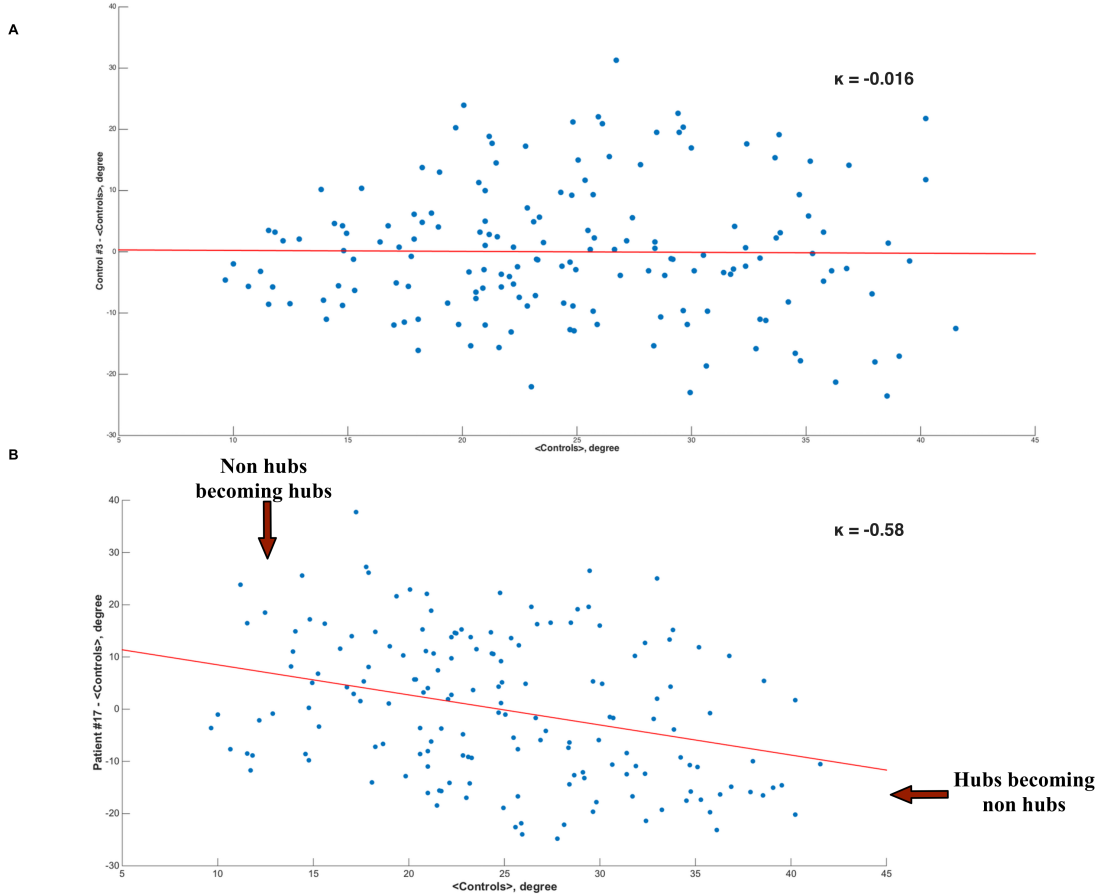
12. Meijer KA, Eijlers AJC, Geurts JGG, et al. Staging of cortical and deep grey matter functional connectivity changes in multiple sclerosis. *J Neurol Neurosurg Psychiatry* 2017; 0: jnnp-2017-316329.
13. Bullmore E, Sporns O. Complex brain networks: graph theoretical analysis of structural and functional systems. *Nat Rev Neurosci* 2009; 10: 312–312.
14. Liu Y, Wang H, Duan Y, et al. Functional Brain Network Alterations in Clinically Isolated Syndrome and Multiple Sclerosis: A Graph-based Connectome Study. *Radiology* 2016; 000: 152843.
15. Shu N, Duan Y, Xia M, et al. Disrupted topological organization of structural and functional brain connectomes in clinically isolated syndrome and multiple sclerosis. *Sci Rep* 2016; 6: 29383.
16. Fleischer V, Radetz A, Ciolac D, et al. Graph theoretical framework of brain networks in multiple sclerosis: A review of concepts. *Neuroscience*. Epub ahead of print 2017. DOI: 10.1016/j.neuroscience.2017.10.033.
17. Eijlers AJC, Meijer KA, Wassenaar TM, et al. Increased default-mode network centrality in cognitively impaired multiple sclerosis patients. *Neurology* 2017; 88: 952–960.
18. Faivre A, Robinet E, Guye M, et al. Depletion of brain functional connectivity enhancement leads to disability progression in multiple sclerosis: A longitudinal resting-state fMRI study. *Mult Scler J* 2016; 22: 1695–1708.
19. Yeo T, Buckner R. The organization of the human cerebral cortex estimated by intrinsic functional connectivity. *J Neurophysiol*, <http://jn.physiology.org.gate2.inist.fr/content/jn/106/3/1125.full.pdf> (2011, accessed 23 May 2017).
20. Achard S, Salvador R, Whitcher B, et al. A Resilient, Low-Frequency, Small-World

- Human Brain Functional Network with Highly Connected Association Cortical Hubs. *J Neurosci* 2006; 26: 63–72.
21. Rubinov M, Sporns O. Complex network measures of brain connectivity: Uses and interpretations. *Neuroimage* 2010; 52: 1059–1069.
 22. Latora V, Marchiori M. Efficient Behavior of Small-World Networks. *Phys Rev Lett* 2001; 87: 198701.
 23. Freeman LC. Centrality in social networks conceptual clarification. *Soc Networks* 1978; 1: 215–239.
 24. Termenon M, Achard S, Jaillard A, et al. The ‘Hub Disruption Index’, a reliable index sensitive to the brain networks reorganization. A study of the contralesional hemisphere in stroke. *Front Comput Neurosci* 2016; 10: 84.
 25. Achard S, Delon-Martin C, Vertes PE, et al. Hubs of brain functional networks are radically reorganized in comatose patients. *Proc Natl Acad Sci* 2012; 109: 20608–20613.
 26. Roosendaal SD, Schoonheim MM, Hulst HE, et al. Resting state networks change in clinically isolated syndrome. *Brain* 2010; 133: 1612–1621.
 27. Roosendaal SD, Schoonheim MM, Hulst HE, et al. Resting state networks change in clinically isolated syndrome. *Brain* 2010; 133: 1612–1621.
 28. Tewarie P, Schoonheim MM, Schouten DI, et al. Functional brain networks: Linking thalamic atrophy to clinical disability in multiple sclerosis, a multimodal fMRI and MEG Study. *Hum Brain Mapp* 2015; 36: 603–618.
 29. Schoonheim MM, Geurts JJG, Barkhof F. The limits of functional reorganization in multiple sclerosis. *Neurology* 2010; 74: 1246–1247.
 30. Tona F, Petsas N, Sbardella E, et al. Multiple sclerosis: Altered Thalamic Resting-State Functional Connectivity and Its Effect on Cognitive Function 1. *Radiol n Radiol*; 271,

- <http://pubs.rsna.org.gate2.inist.fr/doi/pdf/10.1148/radiol.14131688> (2014, accessed 3 November 2017).
31. Hawellek DJ, Hipp JF, Lewis CM, et al. Increased functional connectivity indicates the severity of cognitive impairment in multiple sclerosis. *Proc Natl Acad Sci* 2011; 108: 19066–19071.
 32. Castellazzi G, Debernard L, Melzer TR, et al. Functional Connectivity Alterations Reveal Complex Mechanisms Based on Clinical and Radiological Status in Mild Relapsing Remitting Multiple Sclerosis. *Front Neurol* 2018; 9: 1–15.
 33. Droby A, Yuen KSL, Muthuraman M, et al. Changes in brain functional connectivity patterns are driven by an individual lesion in MS: a resting-state fMRI study. *Brain Imaging Behav* 2016; 10: 1117–1126.
 34. Liu Y, Dai Z, Duan Y, et al. Whole brain functional connectivity in clinically isolated syndrome without conventional brain MRI lesions. *Eur Radiol* 2016; 26: 2982–2991.
 35. Audoin B, Reuter F, Duong MVA, et al. Efficiency of cognitive control recruitment in the very early stage of multiple sclerosis: A one-year fMRI follow-up study. *Mult Scler* 2008; 14: 786–792.
 36. de Reus MA, van den Heuvel MP. The parcellation-based connectome: Limitations and extensions. *Neuroimage* 2013; 80: 397–404.
 37. Hillary FG, Roman CA, Venkatesan U, et al. Hyperconnectivity is a fundamental response to neurological disruption. *Neuropsychology* 2015; 29: 59–75.

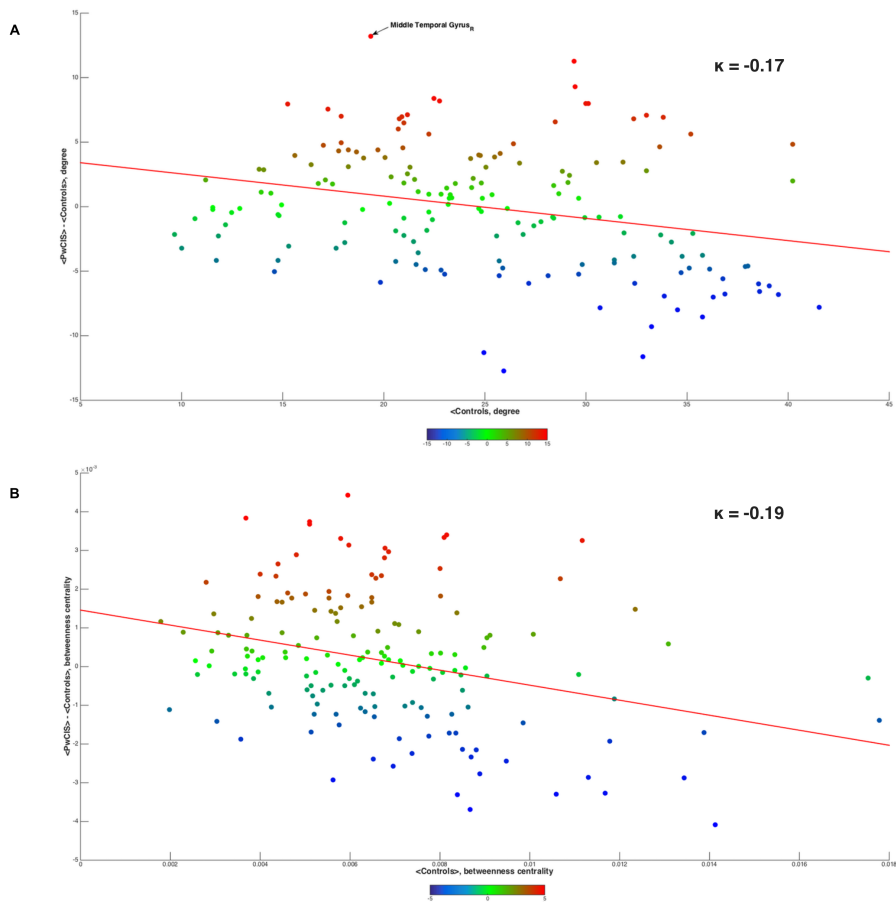
Figure legends

Figure 1. Hub disruption index calculation



Hub disruption index calculation method (of degree) of an individual subject relative to the healthy control group mean for (A) a healthy control subject and (B) a CIS patient subject. To construct the hub disruption index (κ) for the degree, we subtracted the mean degree of the healthy control group for each node from the degree of the corresponding node in an individual subject before plotting this individual difference against the healthy group mean. Each point on this scatterplot represents a node. (κ) is the slope of the red fitted regression line computed on this scatterplot.

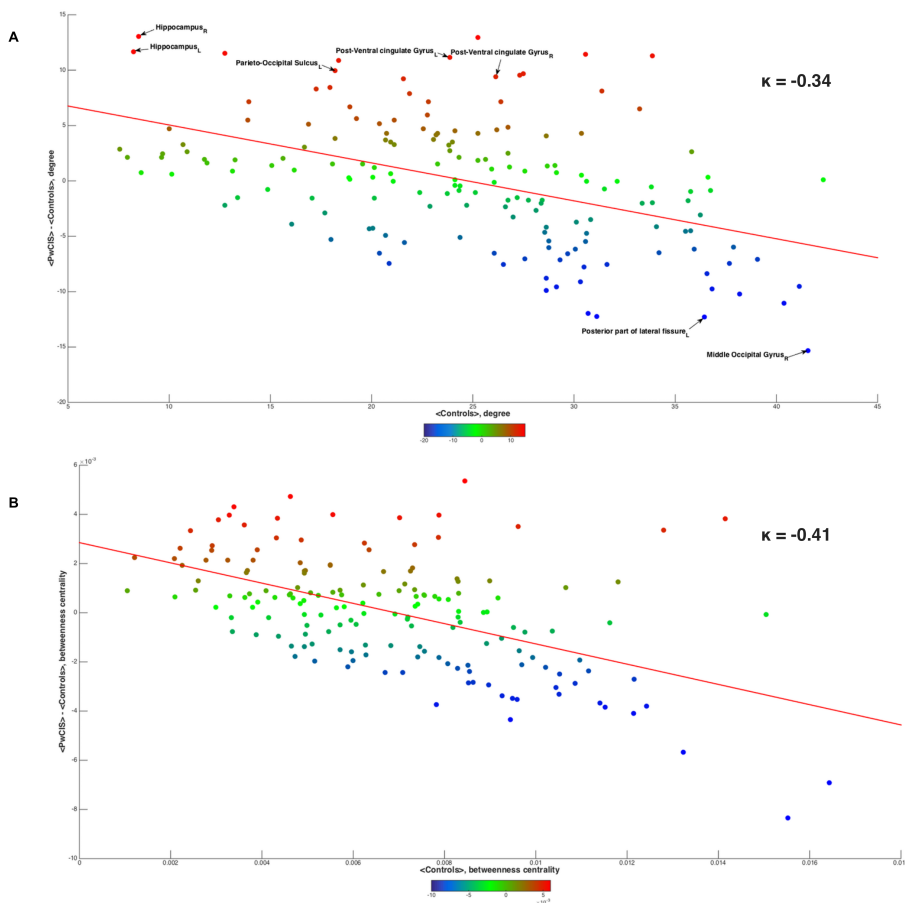
Figure 2. Hub disruption index of PwCIS at baseline



(A) Degree (B) Betweenness centrality

Red denotes increased connectivity measures in the PwCIS compared to HC on average; blue denotes decreased connectivity measures in the PwCIS compared to HC on average.

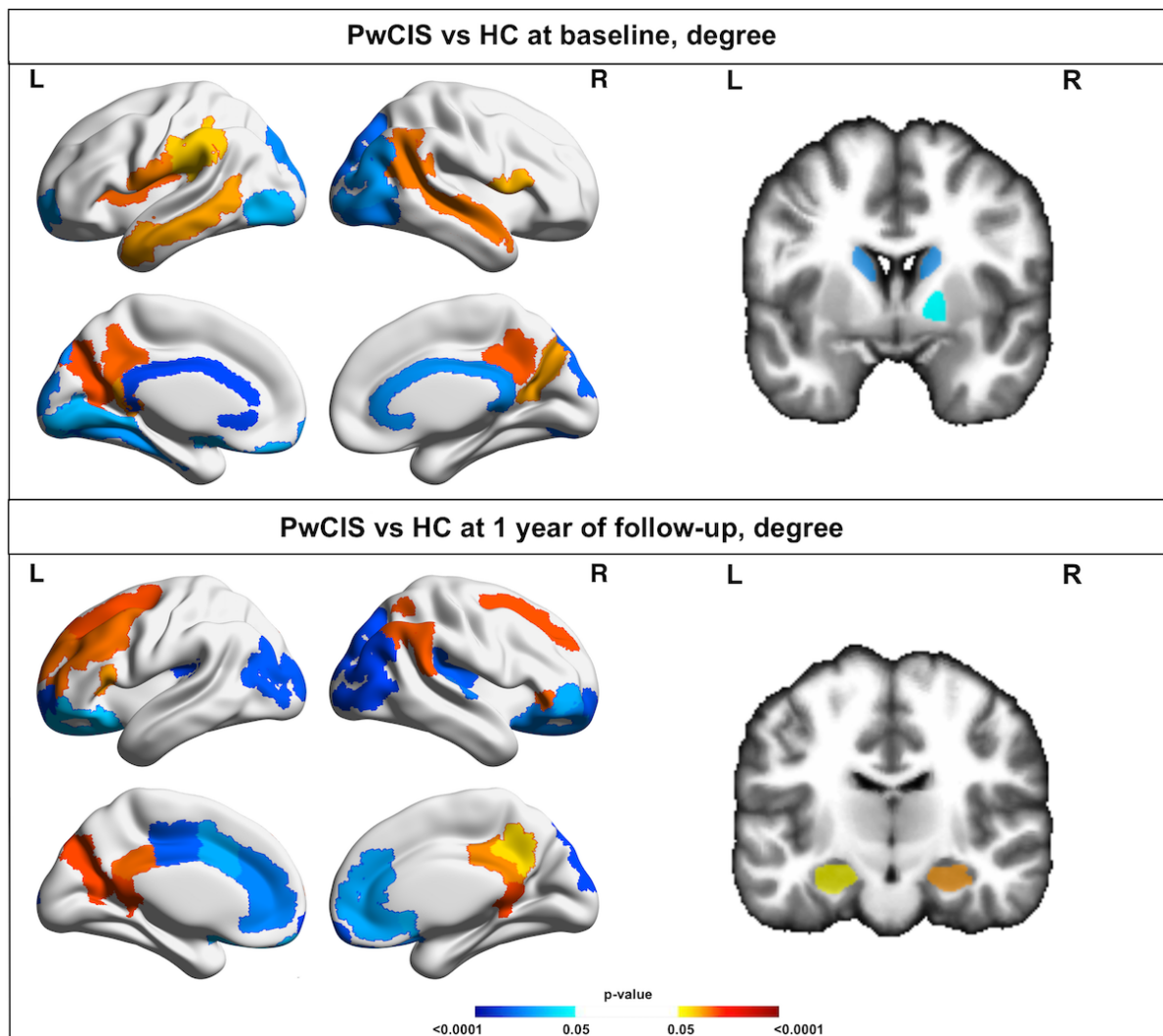
Figure 3. Hub disruption index of PwCIS at 1-year follow-up



(A) Degree (B) Betweenness centrality

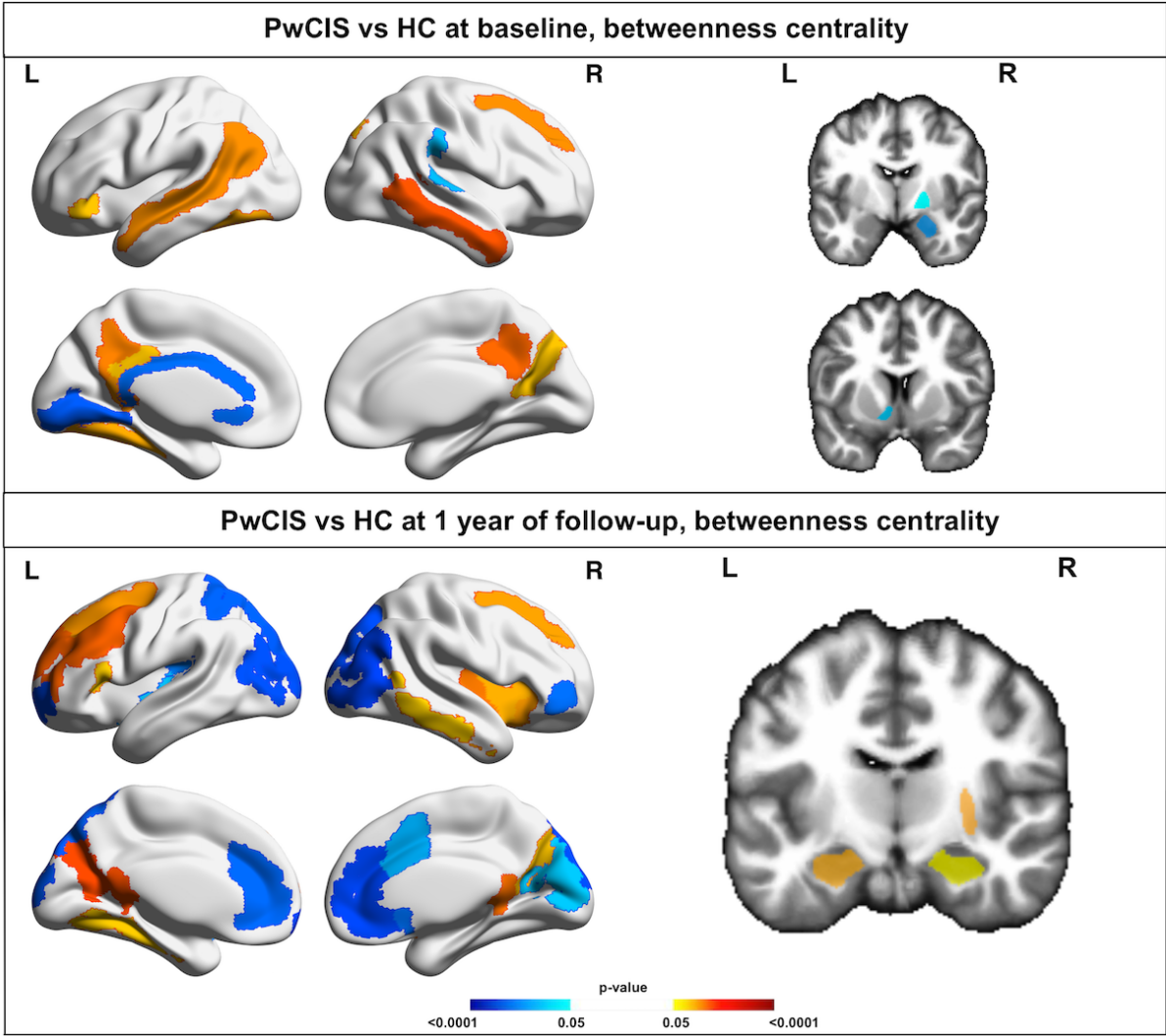
Red denotes increased connectivity measures in the PwCIS compared to HC on average; blue denotes decreased connectivity measures in the PwCIS compared to HC on average.

Figure 4. Regional differences in the nodal degree between PwCIS and HC at baseline and 1 year



Red denotes an increased degree in the PwCIS compared to HC; blue denotes a decreased degree in the PwCIS compared to HC.

Figure 5. Regional differences of betweenness centrality between the PwCIS and HC at baseline and 1 year



Red denotes increased betweenness centrality in the PwCIS compared to HC; blue denotes decreased betweenness centrality in the PwCIS compared to HC.

Table 1. Demographic, Clinical, and Conventional MR Imaging Characteristics

Clinical features	Baseline		Year 1	
	HC (n=19)	CIS (n=41)	HC (n=19)	CIS (n=41)
Mean age, years (SD) ^a	37.8 (8.6)	38.3 (11.2)		
Sex ratio (F/M) ^b	14/5	32/9		
Converters to clinically definite MS (%)	-	-	-	27/41 (66%)
Treatment				
Interferon				10 (24%)
Glatiramer acetate	-	-	-	5 (12%)
Dimethyl fumarate				2 (5%)
Fingolimod				2 (5%)
None				22 (54%)
Education level (high/low) ^c ^b	10/9	26/15		
Mean disease duration (SD) in months	-	4.12 (1.85)		
Median EDSS score [range] ^d	-	1.0 [0-3]	-	1.0 [0-5]
Median T2 Lesion volume (ml) ^d	-	0.98 [0.02-63.12]	-	1.32 [0.07-67.74]

^a Mann-Whitney U test

^b χ^2 test

^c Education level was considered as high or low according to a French baccalaureate.

^d Wilcoxon test to compare PwCIS at baseline and year 1.

Table 2. Location of alterations in functional connectivity

Brain region	Patients vs controls at baseline		Patients vs controls at 1 year	
	Deg	BCN	Deg	BCN
Accumbens	- (L)			
Amygdala		- (R)		
Angular gyrus			+ (R)	
Anterior part of the cingulate gyrus and sulcus			- (L/R)	- (L/R)
Anterior segment of the circular sulcus of the insula				+ (R)
Caudate	- (L/R)			
Collateral sulcus and lingual sulcus	- (L)			+ (L)
Cuneus				- (R)
Fronto-marginal gyrus and sulcus	- (L)		- (L/R)	- (L)
Hippocampus			+ (L/R)	+ (L/R)
Horizontal ramus of the anterior segment of the lateral sulcus			+ (R)	
Inferior occipital gyrus and sulcus	- (L/R)			
Inferior part of the precentral sulcus				
Inferior segment of the circular sulcus of the insula				- (L)
Inferior temporal gyrus				+ (R)
Inferior temporal sulcus				+ (R)
Isthmus of the cingulate gyrus	+ (L)		+ (L/R)	+ (L/R)
Lateral occipito-temporal gyrus		+ (L)		
Lateral orbital sulcus			- (R)	- (R)
Lingual gyrus	- (L)	- (L)		
Long insular gyrus and central sulcus of the insula				+ (R)
Medial orbital sulcus	- (L)			
Middle frontal gyrus			+ (L)	+ (L)
Middle occipital gyrus	- (R)		- (L/R)	- (L/R)
Middle temporal gyrus	+ (L/R)	+ (R)		
Middle-anterior part of the cingulate gyrus and sulcus			- (L)	- (R)

Middle-posterior part of the cingulate gyrus and sulcus			- (L)	
Opercular part of the inferior frontal gyrus	+ (R)			
Orbital gyri			- (L/R)	
Orbital part of the inferior frontal gyrus		+ (L)		
Pallidum	- (R)	- (R)		
Paracentral lobule and sulcus				
Parieto-occipital sulcus	+ (L/R)	+ (R)	+ (L)	+ (L/R)
Pericallosal sulcus	- (L/R)	- (L)		
Planum temporale or temporal plane of the superior temporal gyrus		- (R)		
Posterior segment of the lateral fissure			- (L/R)	- (L)
Posterior transverse collateral sulcus	- (L/R)			
Posterior-dorsal part of the cingulate gyrus		+ (L)	+ (R)	
Putamen				+ (R)
Short insular gyri				+ (R)
Subcallosal gyrus			- (R)	- (R)
Subcentral gyrus and sulci	+ (L)			
Subparietal sulcus	+ (L/R)	+ (L/R)	+ (R)	
Superior frontal sulcus		+ (R)	+ (L/R)	+ (L/R)
Superior occipital gyrus	- (L/R)		- (R)	- (L/R)
Superior occipital sulcus and transverse occipital sulcus		- (R)		
Superior parietal lobule				- (L)
Superior segment of the circular sulcus of the insula	+ (L)			
Superior temporal sulcus	+ (R)	+ (L)		
Supramarginal gyrus	+ (L)			
Transverse temporal sulcus			- (R)	
Vertical ramus of the anterior segment of the lateral sulcus			+ (L)	+ (L)

Deg: degree; BCN: betweenness centrality; R: right; L: left; +: increase in patients compared to controls; -: decrease in patients compared to controls.

Supplementary material

Neuropsychological assessment

We evaluated each cognitive domain with the following tests:

- Attention: Test of Attentional Performance (TAP)¹ consisting of subtests for reaction times (RT) of visual scanning, auditory attention and visual and auditory divided attention. For divided attention, reaction time ratios of the double task (auditory and visual divided attention) to the simple task (auditory or visual attention) was considered.
- Working memory: Paced-Auditory Serial Addition Test-3 s (PASAT).²
- Episodic memory: Selective Reminding Test (SRT),³ which tested verbal memory (three subscores: SRT-LTS=long-term storage; SRT-CLTR=consistent long-term retrieval; SRT-DR=delay recall). Brief Visual Memory Test Revised (BVMTR)⁴ for episodic visuo-spatial memory (two subscores: BVMTR=learning; BVMTR-DR=delay recall).
- Executive functions: Stroop test³ (inhibition task scores) and Word List Generation test³ (verbal fluency assessment).
- Information processing speed (IPS): Computerised Speed Cognitive Test (CSCT)⁵ which is an IPS, a computerised digit-symbol substitution task ⁶ and alertness (with and without warning).

Cognitive status was assessed by z-scores for each test and for both groups (PwCIS and HC) at each time-point to avoid test-retest effect. In order to have a more powerful approach, norms from two in-house studies involving large datasets of HC (N=404 and N=276) were used. Sixteen groups were established according to four age categories (18–34, 34–44, 45–54 and ≥ 55), gender and level of education (low education level (LEL) was below secondary

education, which is usually 12 years of schooling; high education level (HEL) was above secondary education, or graduated at least at a “baccalauréat” level of college degree).

For the cognitive comparison, all of our patients (41 patients) were compared to the initial healthy control group (55 healthy controls) as they all had the neuropsychological assessment.

Table S1: Cognitive performances of clinically isolated syndrome patients and healthy controls at baseline

	HC	CIS	P-value
CSCT	0.25 (0.87)	-0.25 (1.1)	0.04
BVMTR	0.53 (0.8)	0.01 (0.97)	0.006
BVMTR-DR	0.53 (0.53)	-0.11 (1.04)	0.003
PASAT	0.16 (0.94)	0.12 (1.05)	0.93
SRT-LTS	0.42 (1.02)	0.29 (0.93)	0.48
SRT-CLTR	0.34 (1.05)	0.23 (1.07)	0.59
SRT-DR	0.32 (0.69)	0.20 (0.92)	0.95
WLG	-0.30 (0.73)	-0.58 (0.76)	0.07
Alertness	0.49 (0.69)	0.21 (2.55)	0.29
RT_Simple_Visual_Attention	0.24 (0.97)	-0.13 (1.21)	0.43
RT_Simple_Auditory_Attention	0.15 (1.03)	0.16 (1.04)	0.52
RT_Divided_Visual_Attention	-0.51 (1.54)	-0.15 (1.18)	0.28
RT_Divided_Auditory_Attention	-0.04 (1.26)	-0.26 (1.23)	0.31
Stroop	0.03 (0.88)	0.23 (0.84)	0.28

HC: healthy controls; CIS: clinically isolated syndrome; CSCT: computerized speed cognitive test; BVMTR: brief visual memory test revised; DR: delay recall; PASAT: paced auditory serial addition test; SRT: selective reminding test; LTS: long-term storage; CLTR: consistent long-term retrieval; WLG: word list generation; RT: reaction time.

Table S2: Cognitive performances of clinically isolated syndrome patients and healthy controls at 1-year

	HC	CIS	P-value
CSCT	0.43 (1.18)	0.02 (1.04)	0.09
BVMTR	0.44 (0.72)	0.39 (0.89)	0.91
BVMTR-DR	0.22 (0.77)	0.15 (0.89)	0.69
PASAT	0.39 (0.8)	0.36 (0.91)	0.94
SRT-LTS	0.38 (0.75)	0.26 (1.16)	0.65
SRT-CLTR	0.27 (0.98)	0.31 (1.1)	0.85
SRT-DR	0.15 (0.88)	-0.04 (1.06)	0.84
WLG	-0.24 (0.96)	-0.19 (0.98)	0.81
Alertness	0.68 (0.61)	0.25 (1.2)	0.17
RT_Simple_Visual_Attention	0.27 (1.01)	-0.05 (1.1)	0.16
RT_Simple_Auditory_Attention	0.30 (0.91)	-0.07 (1.16)	0.13
RT_Divided_Visual_Attention	0.08 (1.22)	-0.09 (1.27)	0.80
RT_Divided_Auditory_Attention	-0.11 (1.17)	-0.003 (1.33)	0.96
Stroop	0.19 (0.99)	0.35 (1.1)	0.46

HC: healthy controls; CIS: clinically isolated syndrome; CSCT: computerized speed cognitive test; BVMTR: brief visual memory test revised; DR: delay recall; PASAT: paced auditory serial addition test; SRT: selective reminding test; LTS: long-term storage; CLTR: consistent long-term retrieval; WLG: word list generation; RT: reaction time.

MRI acquisition

The MRI acquisition was performed on a 3T MRI system (Achieva TX system, Philips Healthcare, Best, The Netherlands; Signa, GE Healthcare, Discovery MR 750w, Milwaukee, Wisconsin). Resting-state fMRI has been shown to be a reliable imaging marker in multicenter imaging studies as it showed good inter-vendor reliabilities.⁷ The acquisition protocol was harmonized between the magnets and consisted of a three-dimensional (3D) T1-weighted sequence using magnetization prepared rapid gradient echo (MP-RAGE) imaging (TR=8.2 ms, TE=3.5 ms, TI=982 ms, $\alpha=7^\circ$, FOV=256 mm, voxel size=1 mm³, and 180 slices), a two-dimensional (2D) FLAIR sequence (TR=11000 ms, TE=140 ms, TI=2800 ms, FOV=230 mm, 45 axial slices, and 3-mm thick). Additionally, resting-state functional MRI was obtained with an echo-planar imaging (EPI) sequence (250 volumes, 40 axial slices,

TR=2200 ms, TE=30 ms, 3x3-mm in-plane resolution, and slice thickness=3 mm). The first four volumes of the functional run were discarded to achieve steady-state magnetization.

fMRI preprocessing

Using Statistical Parametric Mapping (SPM12, www.fil.ion.ucl.ac.uk/spm), we followed the same fMRI preprocessing that was used in a previous study⁸. Briefly, the constant offset and linear trend over each run were removed and a low-pass temporal filter with a 0.08 Hz cut-off was used, and data were slice time corrected. Sources of spurious variance, as well as their temporal derivatives, were removed through linear regression, including the following: 1) six parameters obtained via correction of rigid body head motion, 2) the signal averaged over the whole brain, 3) the signal averaged over the ventricles, and 4) the signal averaged over the deep cerebral white matter. This regression procedure contributes to the minimization of signal contributions of non-neuronal origin, including respiration-induced signal fluctuations⁹. Registration between the fMRI and the 3D T1 sequences was performed through the use of boundary-based registration and visually checked.

Structural preprocessing and regions of interest

Lesions were segmented on FLAIR data using the Lesion Segmentation Tool (LST) version 2.0.15 (<http://www.applied-statistics.de/lst.html>) in SPM12. Then, they were manually corrected by two blinded experts (IK and CD). Using these maps, a lesion filling algorithm¹⁰ was applied to the T1-weighted images in order to avoid that the lesions affect brain tissue segmentations.

The structural data were preprocessed with the FreeSurfer (v5.3) image analysis suite, which is documented and freely available online (<http://surfer.nmr.mgh.harvard.edu>)¹¹. The brain was separated into regions of interest (ROIs) using a custom-made atlas. The cortical atlas was derived from the Destrieux cortical atlas¹², which is based on a parcellation scheme that

first divides the cortex into gyral and sulcal regions, the limit between both being given by the curvature value of the surface. Deep gray matter (DGM) structures (i.e., the thalamus, hippocampus, pallidus, accumbens, putamen, caudate and amygdala), the cerebellar cortex and the ventral diencephalon (DC), as segmented by FreeSurfer, were also included as ROIs. The complete atlas was then coregistered to each participant's fMRI scan with the inverted boundary-based registration matrix and nearest-neighbor interpolation. The final atlas then segmented the fMRI scan into 83 regions per hemisphere, of which the mean time series were derived.

References:

1. Zimmermann P, Fimm B. Test for attentional performance (TAP). *PsyTest, Herzogenrath*. 1995:76-77. doi:10.1017/CBO9781107415324.004
2. Gronwall DMA. Paced Auditory Serial-Addition Task: A Measure of Recovery from Concussion. *Percept Mot Skills*. 1977;44(2):367-373. doi:10.2466/pms.1977.44.2.367
3. Ruet A, Deloire M, Charre-Morin J, Hamel D, Brochet B. Cognitive impairment differs between primary progressive and relapsing-remitting MS. *Neurology*. 2013;80(16):1501-1508. doi:10.1212/WNL.0b013e31828cf82f
4. Benedict RHB. The Brief Visuospatial Memory Test - Revised. *Psychol Assess*. 1997;(2):145-153. doi:10.1037/1040-3590.8.2.145
5. Ruet A, Deloire MS, Charré-Morin J, Hamel D, Brochet B. A new computerised cognitive test for the detection of information processing speed impairment in multiple sclerosis. *Mult Scler J*. 2013;19(12):1665-1672. doi:10.1177/1352458513480251
6. Smith A. The Symbol-Digit Modalities Test: A neuropsychologic test for economic screening of learning and other cerebral disorders. *Learn Disord*. 1968;3:83-91.
7. An HS, Moon WJ, Ryu JK, et al. Inter-vender and test-retest reliabilities of resting-state functional magnetic resonance imaging: Implications for multi-center imaging studies. *Magn Reson Imaging*. 2017;44:125-130. doi:10.1016/j.mri.2017.09.001
8. Yeo T, Buckner R. The organization of the human cerebral cortex estimated by intrinsic functional connectivity. *J Neurophysiol*. 2011. <http://jn.physiology.org/gate2.inist.fr/content/jn/106/3/1125.full.pdf>. Accessed May 23, 2017.
9. Van Dijk KRA, Hedden T, Venkataraman A, Evans KC, Lazar SW, Buckner RL. Intrinsic Functional Connectivity As a Tool For Human Connectomics: Theory, Properties, and Optimization. *J Neurophysiol*. 2010;103(1):297-321. doi:10.1152/jn.00783.2009
10. Prados F, Cardoso MJ, Kanber B, et al. A multi-time-point modality-agnostic patch-based method for lesion filling in multiple sclerosis. *Neuroimage*. 2016;139:376-384. doi:10.1016/j.neuroimage.2016.06.053
11. Dale AM, Fischl B, Sereno MI. Cortical surface-based analysis: I. Segmentation and surface reconstruction. *Neuroimage*. 1999;9(2):179-194. doi:10.1006/nimg.1998.0395

12. Destrieux C, Fischl B, Dale A, Halgren E. Destrieux C, et al 2010 Automatic parcellation of human cortical gyri and sulci using standard anatomical nomenclature supplemental. *Neuroimage*. 2010;53(1):1-15. doi:10.1016/j.neuroimage.2010.06.010